European Radiology (2019) 29:3584–3594
https://doi.org/10.1007/s00330-018-5947-4

MAGNETIC RESONANCE

T1 mapping for liver function evaluation in gadoxetic acid–enhanced MR imaging: comparison of look-locker inversion recovery and B_1 inhomogeneity–corrected variable flip angle method

Ji Eun Kim[1] · Hyun Ok Kim[2] · Kyungsoo Bae[1] · Dae Seob Choi[1] · Dominik Nickel[3]

Received: 9 October 2018 / Revised: 27 October 2018 / Accepted: 4 December 2018 / Published online: 22 March 2019
© European Society of Radiology 2019

Abstract

Objectives To compare look-locker inversion recovery (LLIR) and B_1 inhomogeneity–corrected variable flip angle T1 mapping methods for estimation of liver function and prediction of hepatic insufficiency and decompensation on gadoxetic acid–enhanced MR imaging.

Methods In this retrospective study, 248 patients with normal liver function, chronic liver disease, or cirrhosis underwent gadoxetic acid–enhanced liver MR imaging, including T1 mapping at 10-min and 20-min hepatobiliary phase (HBP) by using both methods. T1 relaxation times of the liver ($T1_{Liver\text{-}pre}$, $T1_{Liver\text{-}post}$) and the spleen ($T1_{Spleen}$) were correlated between two methods. $\Delta T1_{Liver}$ ([$T1_{Liver\text{-}pre}$ − $T1_{Liver\text{-}post}$]/$T1_{Liver\text{-}pre}$), adjusted $T1_{Liver}$ ([$T1_{Spleen}$ − $T1_{Liver\text{-}post}$]/$T1_{Spleen}$), and functional liver volume-to-weight ratio (liver volume on volumetric T1 map/[$T1_{Liver\text{-}post}$ × patient's weight]) were calculated. The diagnostic performance of T1 parameters and the predictive performance of models (serum marker, serum marker plus T1 parameter) were compared.

Results $T1_{Liver\text{-}post}$ showed a strong correlation ($r = 0.93$, $p < 0.001$) between two methods but was significantly different. For depicting cirrhosis, LLIR-adjusted $T1_{Liver}$ at 10-min HBP showed the highest performance ($p < 0.025$). For predicting hepatic insufficiency and decompensation, LLIR-adjusted $T1_{Liver}$ (Akaike information criterion (AIC), 58.37; C-index, 0.867) and LLIR-$T1_{Liver\text{-}post}$ (AIC, 48.82; C-index, 0.885) at 10-min HBP showed the best performance, respectively, when added to serum albumin level.

Conclusions $T1_{Liver\text{-}post}$ showed a strong correlation between two methods but with significant differences. T1 mapping using LLIR at 10-min HBP with obtainment of adjusted $T1_{Liver}$ and $T1_{Liver\text{-}post}$ may be the best approach for estimation of liver function and prediction of hepatic insufficiency and decompensation.

Key Points

- *$T1_{Liver\text{-}post}$ showed a strong correlation between LLIR and B_1 inhomogeneity–corrected VFA methods, both at 10-min and 20-min HBP but with significant differences.*
- *$T1_{Liver\text{-}post}$ at 10-min and 20-min HBP using LLIR and B_1 inhomogeneity–corrected VFA methods could not be used inter changeably during the follow-up in patients with chronic liver disease (CLD) or cirrhosis.*
- *T1 mapping using LLIR at 10-min HBP with obtainment of adjusted $T1_{Liver}$ and $T1_{Liver\text{-}post}$ may be the most suitable method and parameter for estimation of global liver function and prediction of clinical outcomes in patients with CLD or cirrhosis.*

Keywords Liver · Magnetic resonance imaging · Gadoxetic acid · Cirrhosis

Electronic supplementary material The online version of this article (https://doi.org/10.1007/s00330-018-5947-4) contains supplementary material, which is available to authorized users.

✉ Hyun Ok Kim
galleonok@hanmail.net

[1] Department of Radiology, College of Medicine, Gyeongsang National University, Jinju, Republic of Korea

[2] Department of Internal Medicine, College of Medicine, Gyeongsang National University, 79 Gangnam-ro, Jinju 52727, Republic of Korea

[3] Siemens Healthineers, Erlangen, Germany

Abbreviations

AIC	Akaike information criterion
AUC	Area under the ROC curve
CI	Confidence interval
CLD	Chronic liver disease
CP	Child-Pugh
FLVW	Functional liver volume-to-weight ratio
GRE	Gradient recalled-echo
HBP	Hepatobiliary phase
HCC	Hepatocellular carcinoma
HR	Hazard ratio

LLIR	Look-locker inversion recovery
ROC	Receiver operating characteristic
TE	Echo time
TR	Repetition time
VFA	Variable flip angle

Introduction

Assessment of liver function is important for determining prognosis and management of patients with chronic liver disease (CLD) or cirrhosis [1] who are at increased risk of portal hypertension–related complications and hepatocellular carcinoma (HCC) [2]. In particular, in patients with HCC, evaluation of remnant liver function is essential to minimize risk of postoperative liver failure [3]. Although clinical parameters such as Child-Pugh or Model for End-Stage Liver Disease scores and indocyanine green test are widely used, they are limited to reflect a dynamic state of cirrhosis [4] and to estimate regional liver function [4, 5]. Gadoxetic acid–enhanced liver MR imaging is a unique means to obtain morphological and functional information qualitatively and quantitatively that could improve assessment of both global and regional liver functions [4, 6]. Gadoxetic acid is taken up by hepatocytes through organic anion–transporting polypeptides and excreted into the bile by multidrug-resistant proteins [7], thereby exerting T1 shortening effect on the liver parenchyma [8, 9]. In advanced liver fibrosis, parenchymal enhancement decreases due to the decreased number of functioning hepatocytes or the decreased expression of these transporters [6, 10–12]. However, direct signal measurement is not straightforward because signal varies considerably by imaging parameters or technical factors [5] and it is not linearly related to the gadolinium concentration [13]. To overcome these problems, T1 relaxometry has been suggested as a more reliable method to assess liver function, particularly at 3 T [5]. Among the different T1 mapping methods, look-locker inversion recovery (LLIR) sequence can provide a single-slice high-resolution T1 map within one breath hold [14]. It permits a limited coverage of the liver owing to its long acquisition time [5, 9, 15]. Meanwhile, variable flip angle (VFA) method can obtain a T1 map of the entire liver in a thinner section within one breath hold [6, 8, 16–22]. However, it is more sensitive to B_1 inhomogeneity which causes spatial variations of flip angles and T1 values, particularly when imaging a large field of view at field strengths of 3 T or higher [23, 24]. These two methods have shown the potential for quantitative estimation of liver function [5, 6, 8, 9, 14–17, 20, 22] and prediction of clinical outcomes [14, 21]. However, no interchangeability or comparison has yet been conducted between the two methods in the liver. Recently, B_1 inhomogeneity correction has been available in the VFA method by applying a B_1 mapping pulse sequence before T1 mapping [20, 21]. Interchangeability of T1 values between the LLIR and B_1 inhomogeneity–corrected VFA methods may be important for patient management, as different methods can be used at different times to monitor disease progression in the same patient [9]. Furthermore, finding a more suitable method and T1 parameter in terms of predicting clinical outcomes is needed to allow implementation of optimal preventive management that may modify the natural course of disease in patients with CLD or cirrhosis [2].

Therefore, the purpose of this study was to compare LLIR and B_1 inhomogeneity–corrected VFA T1 mapping methods for estimation of liver function and prediction of hepatic insufficiency and decompensation on gadoxetic acid–enhanced MR imaging.

Materials and methods

Patients

Our institutional review board approved this retrospective study with waiver of informed consent. From October 2016 to January 2018, a total of 330 patients underwent gadoxetic acid–enhanced MR imaging at 3 T for concerns about focal liver lesions. Of these patients, 82 patients were excluded due to the following reasons: (a) diffuse or multinodular hepatic tumors ($n = 47$), (b) motion artifact ($n = 15$), (c) obstructive bile duct dilatation ($n = 13$), (d) splenectomy ($n = 5$), or (e) iron deposition in the T2*-corrected six-echo spoiled gradient recalled-echo (GRE) sequence ($n = 2$). Finally, 248 patients (178 men and 70 women) were included in this study (Fig. 1). Of these patients, 160 were classified as having either Child-Pugh (CP) A cirrhosis ($n = 138$), CP B cirrhosis ($n = 21$), or CP C cirrhosis ($n = 1$) according to surgical resection (F4 fibrosis, $n = 19$, with CP A cirrhosis) or a combination of clinical findings and imaging features ($n = 141$). One hundred fourteen patients with CP A cirrhosis without histopathologic diagnosis had esophageal varix which defines compensated stage 2 cirrhosis [25] on endoscopy within 6 months before or after MR imaging. Thirty-seven patients were regarded as having CLD after surgical resection ($n = 10$: F2 fibrosis [$n = 4$] and F3 fibrosis [$n = 6$]) or according to serologic and sonographic findings without suggestive features of cirrhosis at CT or MRI ($n = 27$). Fifty-one patients were regarded as having normal liver function based on a negative history of liver disease and serologic findings, normal liver function tests, and normal liver stiffness values (mean value, 1.03 m/s ± 0.64 m/s) using elastography point quantification (ElastPQ®). Elastography was performed within 3 months before or after MR imaging. By reviewing the electronic medical records, serum markers examined within 2 weeks of MR imaging were determined, and the development of hepatic insufficiency or decompensation was monitored during the follow-

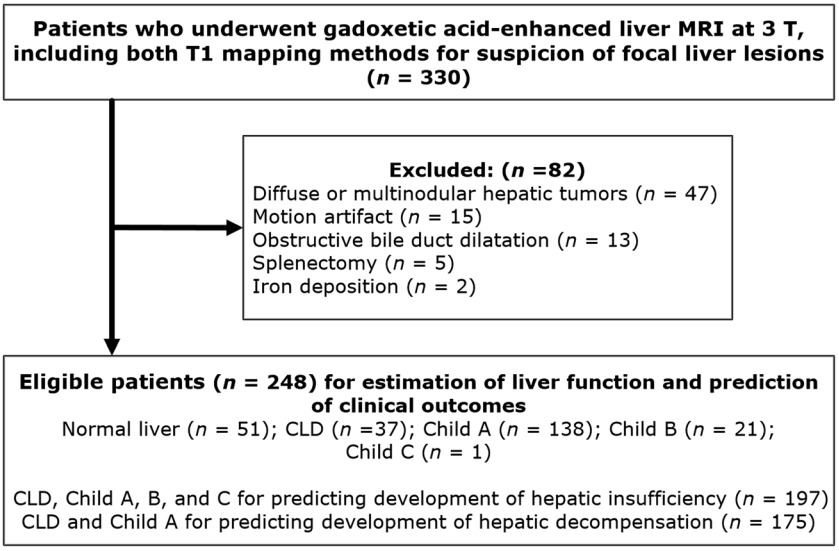

Fig. 1 Flow chart of the study population. CLD, chronic liver disease

up period. Hepatic insufficiency was defined as follows: (a) hepatic encephalopathy, (b) refractory ascites that did not respond to medication, (c) uncontrolled hepatocellular jaundice treated with live transplantation, or (d) death due to hepatic insufficiency. Hepatic decompensation was defined as progression to decompensated cirrhosis (CP B or C) or esophageal variceal bleeding [26, 27]. The patients' characteristics are described in detail in Table 1.

MR imaging

All patients underwent MR imaging on a 3 T unit (Magnetom Skyra; Siemens Healthineers) using a combination of 18-channel body and 12-channel spine matrix coil elements. In addition to routine imaging sequences, T1 maps using LLIR and B_1 inhomogeneity–corrected VFA methods were obtained three times at the precontrast phase and at 10-min and 20-min after the injection of 0.025 mmol of gadoxetic acid (Bayer Healthcare) per kg of body weight at a rate of 1.5 ml/s. For LLIR-T1 map, three axial slices were obtained at the levels of intrahepatic inferior vena cava confluence, portal hilum, and gallbladder fossa. LLIR sequence with a 180° inversion recovery pulse was performed [28] using the following parameters: repetition time (TR)/echo time (TE), 3.0 ms/1.32 ms; flip angle, 8°; number of excitations, 1.0; field of view, 308 mm × 380 mm; matrix, 128 × 113; acceleration factor, 2 using GRAPPA (generalized autocalibrating partially parallel acquisitions); slice thickness, 5 mm; number of images corresponding to the number of data points for voxel-by-voxel fitting procedure, 16; and acquisition time, 3.8 s per slice. For VFA T1 map, T1-weighted volume interpolated breath hold examination (VIBE) sequence with dual flip angles was used with the following parameters: TR/TE, 5.01 ms/2.3 ms; flip angles, 3° and 15°; number of excitations, 1.0; field of view, 305 mm × 379 mm; matrix, 224 × 156; acceleration factor, 4 using CAIPIRINHA (controlled aliasing in parallel imaging results in higher acceleration); slice thickness, 4 mm without intersection gap; and acquisition time, 12 s. To correct B_1 heterogeneity, a B_1 mapping pulse sequence was implemented to acquire a B_1 field map of the entire liver using the stimulated echo/spin echo method [29] before VFA T1 mapping. Inline T1 maps were constructed at the scanner using the software MapIt (Siemens Healthineers).

Image analysis

One gastrointestinal radiologist (*BLINDED*, with 13 years of clinical experience), who was blinded to the clinical results, drew free-hand regions of interest along the margins of the liver and spleen at three slices of both T1 maps, carefully avoiding focal lesions and major branches of the vessels. Each slice had the same anatomic level on both T1 maps (Fig. 2). The mean values of the measured T1 were considered representative T1 relaxation times of the liver ($T1_{Liver\text{-}pre}$, $T1_{Liver\text{-}post}$) and the spleen ($T1_{Spleen}$). Using these values, $\Delta T1_{Liver}$ and adjusted $T1_{Liver}$ were calculated as follows: $\Delta T1_{Liver} = [T1_{Liver\text{-}pre} - T1_{Liver\text{-}post}]/T1_{Liver\text{-}pre}$ [5, 9] and adjusted $T1_{Liver} = [T1_{Spleen} - T1_{Liver\text{-}post}]/T1_{Spleen}$ [14, 30]. In addition, liver volume was calculated on the VFA T1 map as follows: liver volume = sum [area of region of interest × slice thickness]. Then, functional liver volume-to-weight ratio (FLVW) was obtained using the following formula: FLVW = liver volume/[$T1_{Liver\text{-}post}$* × patient's weight] [21]. To reflect the entire liver T1, the median value of all slices containing the liver was used as the representative $T1_{Liver\text{-}post}$* in this formula.

Statistical analysis

Statistical analyses were performed with MedCalc (version 17.9; MedCalc Software) and SAS (version 9.4; SAS Institute, Inc.).

Table 1 Characteristics of the study population

Characteristic	Chronic liver disease ($n = 37$)	Cirrhosis ($n = 160$)
M:F ratio	23:14	125:35
Age*		
Men	59.0 ± 11.2 (33–74)	62.0 ± 9.8 (37–81)
Women	64.9 ± 15.3 (33–84)	68.2 ± 11.1 (38–83)
Weight (kg)*	68.5 ± 12.6 (43–100)	66.7 ± 12.2 (41–120)
Underlying disease		
Hepatitis B virus	20 (54.1)	69 (43.1)
Hepatitis C virus	6 (16.2)	19 (11.9)
Alcoholism	4 (10.8)	60 (37.5)
Coinfection of hepatitis B and C	0 (0)	2 (1.3)
Primary biliary cirrhosis	0 (0)	1 (0.6)
Unknown	7 (18.9)	9 (5.6)
Antiviral medication		
Yes	17 (45.9)	74 (46.3)
Prior medication	3 (8.1)	18 (11.3)
Ongoing medication	14 (37.8)	56 (35.0)
No	20 (54.1)	86 (53.8)
History of HCC		
No	24 (64.9)	71 (55.6)
Yes	13 (35.1)	89 (44.4)
Serum markers*		
Albumin (g/dl)	4.5 ± 0.6 (3.3–7.2)	4.0 ± 0.6 (2.3–6.8)
Total bilirubin (mg/dl)	0.8 ± 0.7 (0.3–4.5)	1.1 ± 1.2 (0.2–9.5)
Prothrombin time (INR)	1.1 ± 0.2 (1.0–2.4)	1.1 ± 0.2 (0.9–1.8)
Child-Pugh class		
A	–	138 (86.3)
B	–	21 (13.1)
C	–	1 (0.6)

Unless otherwise, data in parentheses are percentages

HCC hepatocellular carcinoma, *INR* international normalized ratio

*Data are means ± 1 standard deviation with ranges in parentheses

To evaluate the agreement and relationship for $T1_{Liver}$ and $T1_{Spleen}$ between the two methods, the Bland-Altman analysis [31, 32] and regression analysis were performed, respectively. The Pearson or Spearman's correlation coefficient [33] between the two methods was obtained for four patient groups according to liver function. To evaluate the differences of T1 parameters according to liver function, all T1 parameters at both methods were compared among patient groups using the Kruskal-Wallis test followed by post hoc analysis. Then, we performed a comparison of nonparametric receiver operating characteristic (ROC) curves [34] to compare the diagnostic performance of T1 parameters in depicting cirrhosis from all patients and decompensated cirrhosis from those with cirrhosis. Associations of patient characteristics and T1 parameters with a risk of development of hepatic insufficiency or decompensation were analyzed using the Firth's penalized Cox proportional hazard models [35]. Then, we constructed models with serum marker alone and serum marker plus one T1 parameter. To select the best fit model, the models were compared based on the Akaike information criterion (AIC) [36] and C-index [37]. A detailed description is provided in the Electronic Supplementary Material. P values < 0.05 were considered to indicate statistically significant difference.

Results

Correlation between LLIR-T1 and VFA T1 mapping

The Bland-Altman analysis showed that the mean differences of $T1_{Liver\text{-}post}$ at 10-min and 20-min hepatobiliary phase (HBP) between the two methods were 57.3 (95% confidence interval (CI) = 51.8, 62.7) and 36.7 (95% CI = 31.2, 42.2), respectively. Regression analysis revealed a strong correlation for $T1_{Liver\text{-}post}$ between the two methods, both at 10-min and 20-min HBP ($r = 0.93$, $R^2 = 0.86$ and 0.87, $p < 0.001$) (Fig. 3). The correlation coefficients were 0.826 or more ($p < 0.0001$) in all patient groups

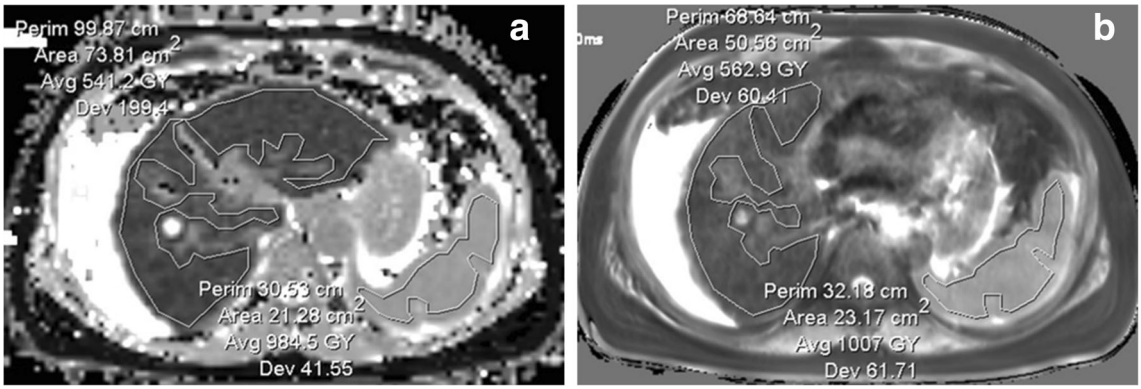

Fig. 2 T1 maps using LLIR sequence (**a**) and B_1 inhomogeneity–corrected VFA method (**b**) obtained at 10-min HBP in a 62-year-old woman with Child-Pugh B. The free-hand drawn regions of interest are shown in the liver and spleen on both T1 maps, which are at the same anatomic level of the portal hilum

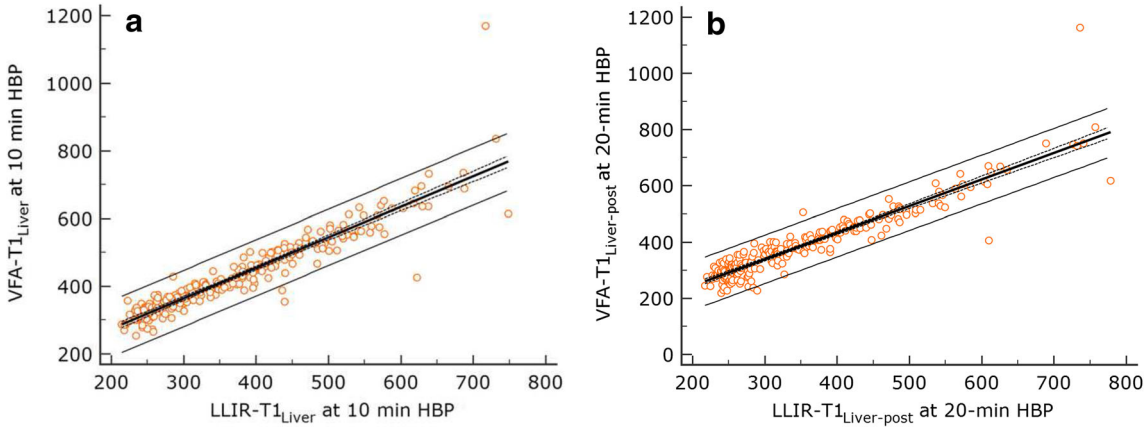

Fig. 3 Scatter diagrams and regression lines of $T1_{Liver\text{-}post}$ at 10-min and 20-min HBP between the LLIR-T1 and VFA T1 mapping methods. Regression equations were as follows: **a** VFA $T1_{Liver\text{-}post}$ at 10-min HBP = 94.346 + [0.902 × LLIR-$T1_{Liver\text{-}post}$ at 10-min HBP], $R^2 = 0.86$, and **b** VFA $T1_{Liver\text{-}post}$ at 20-min HBP = 55.868 + [0.946 × LLIR-$T1_{Liver\text{-}post}$ at 20-min HBP], $R^2 = 0.87$. Thick solid lines = regression line, dashed diverging lines = 95% confidence interval, and solid parallel lines = 95% prediction interval

according to liver function, except for $T1_{Liver\text{-}post}$ at 10-min HBP in patients with CP B or C cirrhosis ($r = 0.764$, $p = 0.0001$) (Table 2). For $T1_{Liver\text{-}pre}$ and $T1_{Spleen}$, regression analysis revealed a moderate correlation between the two methods, both at 10-min and 20-min HBP ($T1_{Liver\text{-}pre}$: $r = 0.68$, $R^2 = 0.41$, $p < 0.001$; $T1_{Spleen}$: $r =$ 0.75 and 0.77, $R^2 = 0.55$ and 0.54, $p < 0.001$) (Table 2).

Diagnostic performance of T1 parameters in identifying cirrhosis and decompensated cirrhosis

$T1_{Liver\text{-}pre}$ and $T1_{Liver\text{-}post}$ significantly increased along with aggravated liver function in all pairwise comparisons ($p < 0.05$) (Table 2, Fig. 4). Similarly, all other T1 parameters significantly decreased with aggravated liver function in all pairwise comparisons ($p < 0.05$) (Table 3), except $T1_{Liver\text{-}pre}$ and $\Delta T1_{Liver}$ between the patient groups of normal liver and CLD. For depicting cirrhosis ($n = 160$, 64.5%) in all 248 patients, LLIR-adjusted $T1_{Liver}$ at 10-min HBP showed the highest diagnostic performance (area under the ROC curve (AUC) = 0.841 [95% CI = 0.789, 0.884]), which was significantly higher than the other T1 parameters (AUC = 0.664–0.815) ($p < 0.025$). For identifying decompensated cirrhosis ($n = 22$, 13.8%) in 160 patients with cirrhosis, LLIR-adjusted $T1_{Liver}$ at 20-min HBP showed the highest diagnostic

Table 2 T1 values of the liver and spleen and their correlation coefficients between LLIR-T1 and VFA T1 mapping according to liver function

T1 values	Normal liver ($n = 51$)	CLD ($n = 37$)	Child-Pugh A ($n = 138$)	Child-Pugh B or C ($n = 22$)	p value*
LLIR-$T1_{Liver\text{-}post}$ at 10-min HBP	279.5 (249.4, 308.2)	290.4 (262.0, 348.3)	394.3 ± 97.0	588.2 ± 95.6	< 0.000001
VFA $T1_{Liver\text{-}post}$ at 10-min HBP	352.8 (317.5, 381.3)	366.8 (336.7, 416.4)	448.6 ± 90.1	590.8 (546.5, 695.2)	< 0.000001
Correlation coefficient	0.890	0.874	0.958	0.764	
LLIR-$T1_{Liver\text{-}post}$ at 20-min HBP	254.7 (245.6, 272.4)	270.9 (248.8, 316.9)	357.8 (284.3, 424.1)	587.1 ± 124.0	< 0.000001
VFA $T1_{Liver\text{-}post}$ at 20-min HBP	300.0 (273.9, 329.6)	322.6 (293.5, 370.4)	397.6 (329.1, 454.0)	566.7 (498.0, 742.2)	< 0.000001
Correlation coefficient	0.880	0.826	0.943	0.833	
LLIR-$T1_{Liver\text{-}pre}$	880.5 ± 69.7	900.6 ± 68.5	952.8 ± 89.4	1054.0 ± 89.7	< 0.001
VFA $T1_{Liver\text{-}pre}$	907.7 ± 60.0	930.8 ± 68.9	960.0 (907.1, 1007.2)	1007.6 (950.5, 1054.0)	0.000008
Correlation coefficient	0.594	0.615	0.633	0.635	
LLIR-$T1_{Spleen}$ at 10-min HBP	951.6 ± 71.5	940.6 ± 68.3	924.3 (862.2, 976.3)	900.3 ± 78.3	0.020099
VFA $T1_{Spleen}$ at 10-min HBP	1007.0 ± 90.2	995.6 ± 90.1	969.1 ± 95.6	936.0 (877.4, 976.1)	0.003065
Correlation coefficient	0.676	0.682	0.800	0.653	
LLIR-$T1_{Spleen}$ at 20-min HBP	1035.8 ± 70.7	1022.1 ± 70.1	1007.9 (952.5, 1059.7)	971.3 ± 83.1	0.005018
VFA $T1_{Spleen}$ at 20-min HBP	1061.7 ± 73.5	1059.4 ± 100.1	1022.5 (967.2, 1073.0)	950.3 (906.2, 1026.7)	0.0000033
Correlation coefficient	0.694	0.700	0.761	0.700	

Data are means ± 1 standard deviation or medians (interquartile range)

LLIR look-locker inversion recovery, *VFA* variable flip angle, *CLD* chronic liver disease, *HBP* hepatobiliary phase

*For the difference in the four different groups

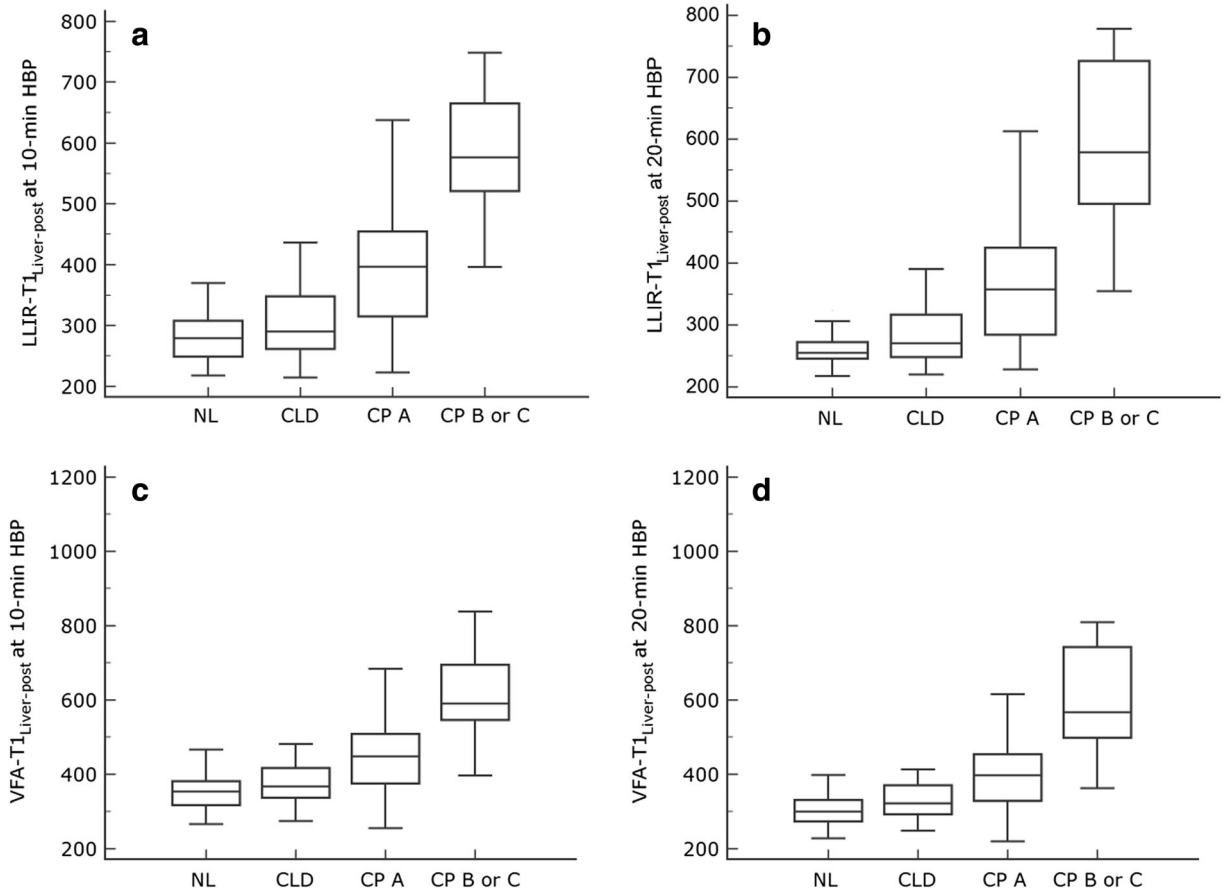

Fig. 4 **a**–**d** Boxplots of $T1_{Liver\text{-}post}$ using LLIR-T1 and VFA T1 mapping methods according to liver function. NL, normal liver; CLD, chronic liver disease; CP, Child-Pugh

performance (AUC = 0.931 [95% CI = 0.880, 0.965]). However, there were no significant differences between this T1 parameter and other T1 parameters (AUC = 0.874–0.923) ($p > 0.05$). The diagnostic performance of T1 parameters did not differ significantly ($p > 0.05$) between the two methods or between 10-min and 20-min HBP, except FLVW.

Table 3 Calculated T1 parameters according to liver function

T1 parameter	Normal liver ($n = 51$)	CLD ($n = 37$)	Child-Pugh A ($n = 138$)	Child-Pugh B or C ($n = 22$)	p value*
LLIR-$\Delta T1_{Liver}$ at 10-min HBP	0.69 (0.64, 0.71)	0.65 ± 0.08	0.59 ± 0.08	0.44 ± 0.07	< 0.000001
LLIR-$\Delta T1_{Liver}$ at 20-min HBP	0.71 (0.69, 0.72)	0.69 (0.64, 0.72)	0.62 ± 0.08	0.45 ± 0.1	< 0.000001
VFA-$\Delta T1_{Liver}$ at 10-min HBP	0.61 ± 0.05	0.59 ± 0.07	0.53 (0.48, 0.6)	0.36 (0.34, 0.42)	< 0.000001
VFA-$\Delta T1_{Liver}$ at 20-min HBP	0.67 ± 0.05	0.64 (0.61, 0.69)	0.58 (0.53, 0.65)	0.44 (0.33, 0.49)	< 0.000001
LLIR-adjusted $T1_{Liver}$ at 10-min HBP	0.71 (0.68, 0.74)	0.69 (0.62, 0.72)	0.58 (0.49, 0.66)	0.34 ± 0.1	< 0.000001
LLIR-adjusted $T1_{Liver}$ at 20-min HBP	0.75 (0.73, 0.77)	0.73 (0.69, 0.76)	0.65 (0.57, 0.72)	0.39 ± 0.13	< 0.000001
VFA-adjusted $T1_{Liver}$ at 10-min HBP	0.65 (0.61, 0.68)	0.63 (0.58, 0.66)	0.54 (0.47, 0.6)	0.34 ± 0.1	< 0.000001
VFA-adjusted $T1_{Liver}$ at 20-min HBP	0.72 (0.68, 0.75)	0.69 (0.64, 0.73)	0.61 (0.54, 0.68)	0.39 ± 0.12	< 0.000001
FLVW at 10-min HBP	0.38 ± 0.08	0.33 ± 0.08	0.29 (0.23, 0.33)	0.17 ± 0.08	< 0.000001
FLVW at 20-min HBP	0.44 ± 0.10	0.38 ± 0.10	0.33 (0.25, 0.38)	0.18 ± 0.08	< 0.000001

Data are means ± 1 standard deviation or medians (interquartile range)

CLD chronic liver disease, *LLIR* look-locker inversion recovery, *HBP* hepatobiliary phase, *VFA* variable flip angle, *FLVW* functional liver volume-to-weight ratio

*For the difference in the four different groups

T1 parameters in association with the development of hepatic insufficiency and decompensation

During the follow-up period (median, 11.5 months; range, 5.2–16.4 months), hepatic insufficiency developed in 9 (4.6%) of 197 patients with CLD or cirrhosis (six men, three women) as follows: hepatic encephalopathy ($n = 4$), death due to hepatic insufficiency ($n = 3$), refractory ascites ($n = 1$), and uncontrolled jaundice ($n = 1$). Hepatic decompensation developed in 8 (4.6%) of 175 patients with CLD or compensated cirrhosis (five men, three women). In the univariate analysis, serum albumin and all T1 parameters showed significant associations with the development of hepatic insufficiency or decompensation (Table 4, $p < 0.05$). The serum albumin level alone model and serum albumin plus one T1 parameter model were selected and compared in the multivariate analysis. Compared with the albumin level alone model, the addition of T1 parameter showed a significant improvement in prediction. Among the models, LLIR-adjusted $T1_{Liver}$ (per 0.1 unit, hazard ratio (HR) = 0.79 [95% CI = 0.67, 0.99], $p = 0.021$, AIC = 58.37, C-index = 0.867) and LLIR-$T1_{Liver\text{-}post}$ (HR = 3.64 [95% CI = 1.54, 9.92], $p = 0.006$, AIC = 48.82, C-index = 0.885) at 10-min HBP showed the best performance in the prediction of hepatic insufficiency and decompensation, respectively, when added to serum albumin level (hepatic insufficiency: per 0.1 unit, HR = 0.81 [95% CI = 0.71, 0.91], $p = 0.001$; hepatic decompensation: per 0.1 unit, HR = 0.78 [95% CI = 0.66, 0.92], $p = 0.004$) (Table 5).

Discussion

In our retrospective study, we found that $T1_{Liver\text{-}post}$ values at 10-min and 20-min HBP using the B_1 inhomogeneity–corrected VFA method were significantly higher than those

Table 4 Univariate cox proportional hazard analysis in association with the development of hepatic insufficiency and decompensation

Characteristic	Hepatic insufficiency		Hepatic decompensation	
	Hazard ratio	*p* value	Hazard ratio	*p* value
Demographic data				
Male sex	1.54 (0.37, 5.43)	0.540	1.91 (0.44, 7.16)	0.373
Age (per 1 year)	1.01 (0.95, 1.07)	0.774	1.02 (0.97, 1.10)	0.469
History of antiviral therapy	2.65 (0.71, 14.17)	0.207	2.66 (0.68, 14.46)	0.216
T1 parameter*				
LLIR-$T1_{Liver\text{-}pre}$ (per 100 units)	3.01 (1.55, 5.97)	0.001	3.39 (1.59, 7.55)	0.002
VFA $T1_{Liver\text{-}pre}$ (per 100 units)	1.72 (0.76, 3.91)	0.194	2.32 (0.94, 5.28)	0.055
LLIR-$T1_{Liver\text{-}post}$ at 10-min HBP (per 100 units)	2.29 (1.40, 3.83)	0.001	5.48 (2.41, 14.57)	< 0.001
LLIR-$T1_{Liver\text{-}post}$ at 20-min HBP (per 100 units)	2.04 (1.36, 3.06)	0.001	3.78 (2.04, 7.48)	< 0.001
VFA $T1_{Liver\text{-}post}$ at 10-min HBP (per 100 units)	1.49 (1.05, 1.89)	0.006	4.72 (2.09, 12.32)	0.001
VFA $T1_{Liver\text{-}post}$ at 20-min HBP (per 100 units)	1.48 (1.09, 1.85)	0.003	3.37 (1.82, 6.45)	< 0.001
LLIR-$\Delta T1_{Liver}$ at 10-min HBP (per 0.1 unit)	0.40 (0.19, 0.79)	0.011	0.21 (0.09, 0.50)	< 0.001
LLIR-$\Delta T1_{Liver}$ at 20-min HBP (per 0.1 unit)	0.42 (0.24, 0.73)	0.002	0.26 (0.13, 0.50)	< 0.001
VFA-$\Delta T1_{Liver}$ at 10-min HBP (per 0.1 unit)	0.62 (0.48, 0.91)	0.003	0.87 (0.34, 1.84)	0.013
VFA-$\Delta T1_{Liver}$ at 20-min HBP (per 0.1 unit)	0.79 (0.67, 1.02)	0.017	0.80 (0.69, 1.02)	0.017
LLIR-adjusted $T1_{Liver}$ at 10-min HBP (per 0.1 unit)	0.68 (0.59, 0.81)	< 0.001	0.69 (0.60, 0.81)	< 0.001
LLIR-adjusted $T1_{Liver}$ at 20-min HBP (per 0.1 unit)	0.47 (0.33, 0.69)	< 0.001	0.33 (0.19, 0.58)	< 0.001
VFA-adjusted $T1_{Liver}$ at 10-min HBP (per 0.1 unit)	0.75 (0.64, 0.95)	0.003	0.74 (0.63, 0.94)	0.002
VFA-adjusted $T1_{Liver}$ at 20-min HBP (per 0.1 unit)	0.77 (0.67, 0.96)	0.003	0.77 (0.67, 0.96)	0.003
FLVW at 10-min HBP (per 0.1 unit)	0.28 (0.13, 0.59)	0.001	0.14 (0.04, 0.40)	0.001
FLVW at 20-min HBP (per 0.1 unit)	0.31 (0.16, 0.59)	0.001	0.18 (0.06, 0.44)	0.001
Laboratory finding*				
Serum albumin (per 0.1 g/dl)	0.78 (0.69, 0.87)	< 0.001	0.75 (0.64, 0.86)	< 0.001
Serum total bilirubin (per 0.1 mg/dl)	1.05 (1.02, 1.07)	< 0.001	1.06 (0.97, 1.11)	0.255
Prothrombin time (per 0.1 INR)	1.40 (1.14, 1.64)	0.127	1.37 (1.02, 1.66)	0.140

Data in parentheses are 95% confidence interval

LLIR look-locker inversion recovery, *VFA* variable flip angle, *HBP* hepatobiliary phase, *FLVW*: functional liver volume-to-weight ratio, *INR* international normalized ratio

*Data in parentheses are reference values

Table 5 Comparison of prediction models in association with the development of hepatic insufficiency and decompensation

Model	Hepatic insufficiency		Hepatic decompensation	
	AIC*	C-index**	AIC*	C-index**
Serum albumin	63.67	0.867 (0.794, 0.939)	57.59	0.784 (0.586, 0.981)
Serum albumin + LLIR-$T1_{Liver\text{-}pre}$	62.34	0.876 (0.81, 0.943)	51.40	0.855 (0.726, 0.985)
Serum albumin + VFA $T1_{Liver\text{-}pre}$	63.45	0.869 (0.804, 0.934)	56.91	0.794 (0.610, 0.977)
Serum albumin + LLIR-$T1_{Liver\text{-}post}$ at 10-min HBP	63.51	0.864 (0.793, 0.935)	48.82	0.885 (0.809, 0.960)
Serum albumin + LLIR-$T1_{Liver\text{-}post}$ at 20-min HBP	63.02	0.865 (0.794, 0.936)	49.86	0.872 (0.785, 0.959)
Serum albumin + VFA $T1_{Liver\text{-}post}$ at 10-min HBP	62.74	0.878 (0.815, 0.941)	51.00	0.880 (0.797, 0.964)
Serum albumin + VFA $T1_{Liver\text{-}post}$ at 20-min HBP	62.74	0.867 (0.795, 0.939)	52.17	0.845 (0.727, 0.962)
Serum albumin + LLIR-$\Delta T1_{Liver}$ at 10-min HBP	64.17	0.865 (0.791, 0.939)	52.55	0.870 (0.787, 0.953)
Serum albumin + LLIR-$\Delta T1_{Liver}$ at 20-min HBP	63.72	0.866 (0.794, 0.938)	51.33	0.872 (0.781, 0.963)
Serum albumin + VFA-$\Delta T1_{Liver}$ at 10-min HBP	62.90	0.865 (0.794, 0.936)	57.07	0.766 (0.540, 0.992)
Serum albumin + VFA-$\Delta T1_{Liver}$ at 20-min HBP	62.85	0.865 (0.794, 0.936)	53.30	0.821 (0.667, 0.975)
Serum albumin + LLIR-adjusted $T1_{Liver}$ at 10-min HBP	58.37	0.873 (0.800, 0.947)	52.04	0.855 (0.716, 0.993)
Serum albumin + LLIR-adjusted $T1_{Liver}$ at 20-min HBP	61.80	0.864 (0.793, 0.936)	52.81	0.838 (0.704, 0.972)
Serum albumin + VFA-adjusted $T1_{Liver}$ at 10-min HBP	62.83	0.862 (0.787, 0.936)	55.32	0.800 (0.622, 0.977)
Serum albumin + VFA-adjusted $T1_{Liver}$ at 20-min HBP	62.98	0.854 (0.772, 0.936)	53.61	0.808 (0.644, 0.972)
Serum albumin + FLVW at 10-min HBP	63.64	0.862 (0.782, 0.941)	52.90	0.852 (0.706, 0.999)
Serum albumin + FLVW at 20-min HBP	62.93	0.866 (0.789, 0.944)	53.24	0.799 (0.615, 0.983)

Data in parentheses are 95% confidence intervals

AIC Akaike information criterion, *LLIR* look-locker inversion recovery, *HBP* hepatobiliary phase, *FLVW* functional liver volume-to-weight ratio

*The lowest AIC value **The highest C-index value means the best model

using the LLIR method ($p < 0.001$), with mean differences of 57.3 and 36.7, respectively. These results are consistent with those of previous study [24], in which the LLIR method produced lower T1 values on average compared with the B_1 inhomogeneity–corrected VFA method in the brain white matter of phantom and healthy patients. As far as we know, there are no comparison studies between the two methods in the liver. In addition, according to our results, $T1_{Liver\text{-}post}$ showed a strong correlation ($r \geq 0.826$) between the two methods, both at 10-min and 20-min HBP in all patient groups, except $T1_{Liver\text{-}post}$ at 10-min HBP in patients with decompensated cirrhosis. Therefore, $T1_{Liver\text{-}post}$ at 10-min and 20-min HBP using the LLIR and B_1 inhomogeneity–corrected VFA methods could not be used interchangeably during the follow-up after treatment in patients with CLD or cirrhosis, as well as in those with normal liver function. This is especially the case in patients with decompensated cirrhosis in whom $T1_{Liver\text{-}post}$ at 10-min HBP showed a moderate correlation ($r = 0.764$) between the two methods. It can be explained by the increased effect of $T1_{Liver\text{-}pre}$ on the $T1_{Liver\text{-}post}$ at 10-min HBP in this poor liver function group with decreased contrast uptake because $T1_{Liver\text{-}pre}$ in this group showed a moderate correlation ($r = 0.635$) between the two methods. We also found that $T1_{Liver\text{-}pre}$ and $T1_{Spleen}$ showed a moderate correlation ($T1_{Liver\text{-}pre}$: $r = 0.68$, $T1_{Spleen}$: $r = 0.75$ and 0.77) between the two methods in all patients. The effect of gadoxetic acid on the $T1_{Liver\text{-}post}$ at HBP may be larger than that of imperfect spoiling and B_1 inhomogeneity which account for differences in T1 values between the two methods [24], and it may explain a better correlation of $T1_{Liver\text{-}post}$ than that of $T1_{Liver\text{-}pre}$ or$T1_{Spleen}$ between the two methods in our study. Among the different T1 mapping methods, the LLIR and VFA methods can be easily incorporated into routine liver MR imaging and have already shown the potential for quantitative estimation of liver function in previous studies [5, 6, 8, 9, 14–17, 20, 21]. Therefore, these two methods can be used to monitor patients during the follow-up in the era of antifibrotic treatment, which may delay progression to decompensated cirrhosis or even reverse cirrhosis [38]. However, we suggest caution when using different methods during the follow-up because the two methods could not be interchangeable in the present study.

We also compared the clinical impact of both methods comprehensively using various T1 parameters reported in the literatures and serum markers at the two most widely used acquisition times. According to our results, LLIR-adjusted $T1_{Liver}$ at 10-min HBP showed the best performance in predicting the development of hepatic insufficiency, when added to serum albumin level, and it also showed the highest diagnostic performance in depicting cirrhosis. For predicting

the occurrence of hepatic decompensation, LLIR-$T1_{Liver\text{-}post}$ at 10-min HBP showed the best performance. Therefore, we propose that T1 mapping using LLIR at 10-min HBP with obtainment of adjusted $T1_{Liver}$ and LLIR-$T1_{Liver\text{-}post}$ could be the most suitable method and parameter for estimation of liver function and prediction of clinical outcomes in patients with CLD or cirrhosis. In addition, the LLIR method and 10-min HBP generally showed better performance than the VFA method and 20-min HBP, respectively, for the top five parameters with lower AIC values for prediction of hepatic insufficiency and decompensation. Previous researchers [22] reported that 10-min HBP showed similar diagnostic performance to 20-min HBP for liver function assessment. These results can be meaningful in clinical practice in terms of decreased time for imaging acquisition and analysis because acquisition of T1 mapping at the precontrast phase can be omitted, acquisition at 10-min HBP does not need additional scan time, and measurement of many sections of the VFA T1 map is not necessary to reflect the entire liver T1 or to obtain the liver volume. Unlike previous studies reporting that the addition of liver volume assessment showed a stronger correlation with liver function than the VFA $T1_{Liver\text{-}post}$ [20] or $\Delta T1_{Liver}$ [8, 20], FLVW generally did not show better performance compared to $T1_{Liver\text{-}post}$ or LLIR-adjusted $T1_{Liver}$ in the present study. A previous study [21] also noted that VFA $T1_{Liver\text{-}post}$ was superior to FLVW for prediction of hepatic insufficiency. This can be explained by imperfect volume estimation on the VFA T1 map. In some cases of our study, measurement of the left lobe was avoided at sections just below the heart due to motion artifacts. This artifact should be resolved in the future at the present B_1 inhomogeneity–corrected VFA method. The best performance of LLIR-adjusted $T1_{Liver}$ in our study can be explained by the use of $T1_{Spleen}$ and LLIR method. $T1_{Spleen}$ corrects effects of extracellular contrast enhancement on the $T1_{Liver\text{-}post}$, and this may enable adjusted $T1_{Liver}$ to reflect T1 shortening by intracellular gadoxetic acid [14, 30]. Unlike the LLIR method that uses an inversion pulse, the VFA method that uses the consecutive spoiled GRE sequences at least two different flip angles is more vulnerable to incomplete spoiling and B_1 inhomogeneity because radiofrequency spoiling is standard for the spoiled GRE sequence and flip angles depends on the B_1 homogeneity [23, 24]. Therefore, incomplete spoiling and B_1 bias, which are not completely resolved by conventional hardware and techniques in 3 T even after B_1 inhomogeneity correction, can result in more biased T1 values at the VFA method [24], thereby weakening the performance of T1 parameters at this method. In the study by Yoon et al [14] evaluating $T1_{Liver}$, $\Delta T1_{Liver}$, and adjusted $T1_{Liver}$ using the LLIR method, only adjusted $T1_{Liver}$ was significantly associated with the presence of varices [24]. Furthermore, our values of $T1_{Liver\text{-}post}$ [9, 14, 15] and adjusted $T1_{Liver}$ [14] using the LLIR method were similar to those in previous studies. Therefore, we believe performing the LLIR method at 10-min HBP with obtainment of adjusted $T1_{Liver}$ and $T1_{Liver\text{-}post}$ may be useful in clinical settings in which different MR imaging units are used. At present, T1 estimations should be considered as method-dependent and may be even system- and configuration-dependent [39]. Further studies that include vendor collaboration and multisite trials are warranted to determine vendor variations and to develop a universal scheme for T1 mapping in patients with CLD or cirrhosis.

There are several limitations in our study. First, because it was a retrospective, single institution study, a certain degree of selection bias was inevitable. Second, relatively short follow-up period and a small number of progression cases may limit statistical reliability due to large mean squared error [40]. However, our results are consistent with the rates of cirrhosis progression in previous articles [21, 41]. In addition, the sample size in the present study may not be large enough for definite conclusion to be extrapolated to all subgroups of patients according to the severity or etiology of cirrhosis. Third, our study was performed using the same MR imaging unit. Therefore, it may not be possible to extrapolate our results to a clinical situation in which different MR imaging units are used. Thus, larger longitudinal studies with various etiologies of cirrhosis and MR imaging units are needed. Fourth, the histopathologic diagnosis was not available for the majority of patients, and some patients may be misclassified as having CLD versus CP A cirrhosis. Finally, we did not evaluate intra- and interobserver agreement. However, our measurement of the entire liver and spleen may minimize sampling bias related to intra- and interobserver variation.

In conclusion, $T1_{Liver\text{-}post}$ showed a strong correlation between the LLIR and B_1 inhomogeneity–corrected VFA methods but with significant differences. T1 mapping using LLIR at 10-min HBP with obtainment of adjusted $T1_{Liver}$ and $T1_{Liver\text{-}post}$ may be the best approach for estimation of liver function and prediction of hepatic insufficiency and decompensation.

Funding The authors state that this work has not received any funding.

Compliance with ethical standards

Guarantor The scientific guarantor of this publication is Hyun Ok Kim.

Conflict of interest The authors declare that they have no conflict of interest.

Statistics and biometry Professor Kim Rock Bum kindly provided statistical advice for this manuscript.

Informed consent Written informed consent was waived by the Gyeongsang National University Hospital Institutional Review Board.

Ethical approval Gyeongsang National University Hospital Institutional Review Board approval was obtained.

Methodology
- retrospective
- diagnostic or prognostic study
- performed at one institution

References

1. Zipprich A, Kuss O, Rogowski S et al (2010) Incorporating indocyanin green clearance into the model for end stage liver disease (MELD-ICG) improves prognostic accuracy in intermediate to advanced cirrhosis. Gut 59:963–968
2. Singh S, Fujii LL, Murad MH et al (2013) Liver stiffness is associated with risk of decompensation, liver cancer, and death in patients with chronic liver diseases: a systematic review and meta-analysis. Clin Gastroenterol Hepatol 11:1573–1584 e1571–1572; quiz e1588–1579
3. Belghiti J, Ogata S (2005) Assessment of hepatic reserve for the indication of hepatic resection. J Hepatobiliary Pancreat Surg Surg 12:1–3
4. Ba-Ssalamah A, Bastati N, Wibmer A et al (2017) Hepatic gadoxetic acid uptake as a measure of diffuse liver disease: where are we? J Magn Reson Imaging 45:646–659
5. Katsube T, Okada M, Kumano S et al (2011) Estimation of liver function using T1 mapping on Gd-EOB-DTPA-enhanced magnetic resonance imaging. Invest Radiol 46:277–283
6. Besa C, Bane O, Jajamovich G, Marchione J, Taouli B (2015) 3D T1 relaxometry pre and post gadoxetic acid injection for the assessment of liver cirrhosis and liver function. Magn Reson Imaging 33: 1075–1082
7. Van Beers BE, Pastor CM, Hussain HK (2012) Primovist, Eovist: what to expect? J Hepatol 57:421–429
8. Yoneyama T, Fukukura Y, Kamimura K et al (2014) Efficacy of liver parenchymal enhancement and liver volume to standard liver volume ratio on Gd-EOB-DTPA-enhanced MRI for estimation of liver function. Eur Radiol 24:857–865
9. Haimerl M, Verloh N, Zeman F et al (2013) Assessment of clinical signs of liver cirrhosis using T1 mapping on Gd-EOB-DTPA-enhanced 3T MRI. PLoS One 8:e85658
10. Lagadec M, Doblas S, Giraudeau C et al (2015) Advanced fibrosis: correlation between pharmacokinetic parameters at dynamic gadoxetate-enhanced MR imaging and hepatocyte organic anion transporter expression in rat liver. Radiology 274:379–386
11. Hinoshita E, Taguchi K, Inokuchi A et al (2001) Decreased expression of an ATP-binding cassette transporter, MRP2, in human livers with hepatitis C virus infection. J Hepatol 35:765–773
12. Sheng RF, Wang HQ, Yang L et al (2017) Assessment of liver fibrosis using T1 mapping on Gd-EOB-DTPA-enhanced magnetic resonance. Dig Liver Dis 49:789–795
13. Materne R, Smith AM, Peeters F et al (2002) Assessment of hepatic perfusion parameters with dynamic MRI. Magn Reson Med 47: 135–142
14. Yoon JH, Lee JM, Paek M, Han JK, Choi BI (2016) Quantitative assessment of hepatic function: modified look-locker inversion recovery (MOLLI) sequence for T1 mapping on Gd-EOB-DTPA-enhanced liver MR imaging. Eur Radiol 26:1775–1782
15. Nakagawa M, Namimoto T, Shimizu K et al (2017) Measuring hepatic functional reserve using T1 mapping of Gd-EOB-DTPA enhanced 3T MR imaging: a preliminary study comparing with (99m)Tc GSA scintigraphy and signal intensity based parameters. Eur J Radiol 92:116–123
16. Kamimura K, Fukukura Y, Yoneyama T et al (2014) Quantitative evaluation of liver function with T1 relaxation time index on Gd-EOB-DTPA-enhanced MRI: comparison with signal intensity-based indices. J Magn Reson Imaging 40:884–889
17. Ding Y, Rao SX, Chen C, Li R, Zeng MS (2015) Assessing liver function in patients with HBV-related HCC: a comparison of T(1) mapping on Gd-EOB-DTPA-enhanced MR imaging with DWI. Eur Radiol 25:1392–1398
18. Ding Y, Rao SX, Zhu T, Chen CZ, Li RC, Zeng MS (2015) Liver fibrosis staging using T1 mapping on gadoxetic acid-enhanced MRI compared with DW imaging. Clin Radiol 70: 1096–1103
19. Yang L, Ding Y, Rao S et al (2017) Staging liver fibrosis in chronic hepatitis B with T1 relaxation time index on gadoxetic acid-enhanced MRI: comparison with aspartate aminotransferase-to-platelet ratio index and FIB-4. J Magn Reson Imaging 45:1186–1194
20. Haimerl M, Schlabeck M, Verloh N et al (2016) Volume-assisted estimation of liver function based on Gd-EOB-DTPA-enhanced MR relaxometry. Eur Radiol 26:1125–1133
21. Yoon JH, Lee JM, Kim E, Okuaki T, Han JK (2017) Quantitative liver function analysis: volumetric T1 mapping with fast multisection B1 inhomogeneity correction in hepatocyte-specific contrast-enhanced liver MR imaging. Radiology 282:408–417
22. Zhou ZP, Long LL, Qiu WJ et al (2017) Comparison of 10- and 20-min hepatobiliary phase images on Gd-EOB-DTPA-enhanced MRI T1 mapping for liver function assessment in clinic. Abdom Radiol (NY) 42:2272–2278
23. Treier R, Steingoetter A, Fried M, Schwizer W, Boesiger P (2007) Optimized and combined T1 and B1 mapping technique for fast and accurate T1 quantification in contrast-enhanced abdominal MRI. Magn Reson Med 57:568–576
24. Stikov N, Boudreau M, Levesque IR, Tardif CL, Barral JK, Pike GB (2015) On the accuracy of T1 mapping: searching for common ground. Magn Reson Med 73:514–522
25. Asrani SK, Kamath PS (2013) Natural history of cirrhosis. Curr Gastroenterol Rep 15:308
26. Poynard T, Vergniol J, Ngo Y et al (2014) Staging chronic hepatitis C in seven categories using fibrosis biomarker (FibroTest) and transient elastography (FibroScan®). J Hepatol 60:706–714
27. Asrani SK, Talwalkar JA, Kamath PS et al (2014) Role of magnetic resonance elastography in compensated and decompensated liver disease. J Hepatol 60:934–939
28. Deichmann R, Hasse A (1992) Quantification of T1 values by SNAPSHOT-FLASH NMR imaging. J Magn Reson 96: 608–612
29. Perman WH, Bernstein MA, Sandstrom JC (1989) A method for correctly setting the rf flip angle. Magn Reson Med 9:16–24
30. Yamada A, Hara T, Li F et al (2011) Quantitative evaluation of liver function with use of gadoxetate disodium-enhanced MR imaging. Radiology 260:727–733
31. Bland JM, Altman DG (1995) Comparing methods of measurement: why plotting difference against standard method is misleading. Lancet 346:1085–1087
32. Bland JM, Altman DG (1986) Statistical methods for assessing agreement between two methods of clinical measurement. Lancet 1:307–310
33. Zou KH, Tuncali K, Silverman SG (2003) Correlation and simple linear regression. Radiology 227:617–622
34. Park SH, Goo JM, Jo CH (2004) Receiver operating characteristic (ROC) curve: practical review for radiologists. Korean J Radiol 5:11–18
35. Firth D (1993) Bias reduction of maximum likelihood estimates. Biometrika 80:27–38
36. Burnham KP, Anderson DR (2004) Multimodel inference: understanding AIC and BIC in model selection. Sociol Methods Res 33: 261–304
37. Harrell FE Jr, Lee KL, Mark DB (1996) Multivariable prognostic models: issues in developing models, evaluating assumptions and adequacy, and measuring and reducing errors. Stat Med 15:361–387

38. Schuppan D, Kim YO (2013) Evolving therapies for liver fibrosis. J Clin Invest 123:1887–1901
39. Liberman G, Louzoun Y, Ben Bashat D (2014) T(1) mapping using variable flip angle SPGR data with flip angle correction. J Magn Reson Imaging 40:171–180
40. King G, Zeng L (2001) Logistic regression in rare events data. Polit Anal 9:137–163
41. D'Amico G, Garcia-Tsao G, Pagliaro L (2006) Natural history and prognostic indicators of survival in cirrhosis: a systematic review of 118 studies. J Hepatol 44:217–231

Publisher's note Springer Nature remains neutral with regard to jurisdictional claims in published maps and institutional affiliations.